




# Bispecific immune cell engager enhances the anticancer activity of CD16<sup>+</sup> NK cells and macrophages in vitro, and eliminates cancer metastasis in NK humanized NOG mice

Shahryar Khoshtinat Nikkhai <sup>1</sup>, Ge Yang,<sup>1</sup> Hajar Owji,<sup>1</sup> Mayara Grizotte-Lake,<sup>2</sup> Rick I Cohen,<sup>1</sup> Lazaro Gil Gonzalez <sup>3</sup>, Mohammad Massumi,<sup>1</sup> Arash Hatefi <sup>1,4</sup>

**To cite:** Khoshtinat Nikkhai S, Yang G, Owji H, *et al.* Bispecific immune cell engager enhances the anticancer activity of CD16<sup>+</sup> NK cells and macrophages in vitro, and eliminates cancer metastasis in NK humanized NOG mice. *Journal for ImmunoTherapy of Cancer* 2024;**12**:e008295. doi:10.1136/jitc-2023-008295

► Additional supplemental material is published online only. To view, please visit the journal online (<https://doi.org/10.1136/jitc-2023-008295>).

Accepted 28 February 2024



© Author(s) (or their employer(s)) 2024. Re-use permitted under CC BY-NC. No commercial re-use. See rights and permissions. Published by BMJ.

<sup>1</sup>Rutgers, The State University of New Jersey, Piscataway, New Jersey, USA

<sup>2</sup>Taconic Biosciences Inc, Germantown, New York, USA

<sup>3</sup>St Michael's Hospital Keenan Research Centre for Biomedical Science, Toronto, Ontario, Canada

<sup>4</sup>Rutgers Cancer Institute of New Jersey, New Brunswick, New Jersey, USA

## Correspondence to

Professor Arash Hatefi; [ahatefi@pharmacy.rutgers.edu](mailto:ahatefi@pharmacy.rutgers.edu)

## ABSTRACT

**Background** In a prior report, we detailed the isolation and engineering of a bispecific killer cell engager, referred to as BiKE:E5C1. The BiKE:E5C1 exhibits high affinity/specificity for the CD16a activating receptor on natural killer (NK) cells and human epidermal growth factor receptor 2 (HER2) on cancer cells. In vitro studies have demonstrated that BiKE:E5C1 can activate the NK cells and induce the killing of HER2<sup>+</sup> ovarian and breast cancer cells, surpassing the performance of the best-in-class monoclonal antibody, Trazimera (trastuzumab). To advance this BiKE technology toward clinical application, the objective of this research was to demonstrate the ability of BiKE:E5C1 to activate CD16<sup>+</sup> immune cells such as NK cells and macrophages to kill cancer cells, and eradicate metastatic HER2<sup>+</sup> tumors in NK humanized NOG mice.

**Methods** We assessed BiKE:E5C1's potential to activate CD16<sup>+</sup>-expressing peripheral blood (PB)-NK cells, laNK92 cells, and THP-1-CD16A monocyte-macrophages through flowcytometry and antibody-dependent cell-mediated cytotoxicity/phagocytosis (ADCC) assays. Subsequently, laNK92 cells were selected as effector cells and genetically modified to express the nanoluciferase gene, enabling the monitoring of their viability in NK humanized NOG mice using quantitative bioluminescent imaging (qBLI). To evaluate the functionality of BiKE:E5C1 in vivo, we introduced firefly luciferase-expressing ovarian cancer cells via intraperitoneal injection into hIL-15 and hIL-2 NOG mice, creating a model of ovarian cancer metastasis. Once tumor establishment was confirmed, we treated the mice with laNK92 cells plus BiKE:E5C1 and the response to therapy was assessed using qBLI.

**Results** Our data demonstrate that BiKE:E5C1 activates not only laNK92 cells but also PB-NK cells and macrophages, significantly enhancing their anticancer activities. ADCC assay demonstrated that IgG, Fc region had no impact on BiKE:E5C1's anticancer activity. In vivo results reveal that both hIL-15 and hIL-2 NOG mouse models support the viability and proliferation of laNK92 cells. Furthermore, it was observed that BiKE:E5C1 activates laNK92 cells in mice, leading to eradication of cancer metastasis in both NK humanized hIL-15 and hIL-2 NOG mouse models.

## WHAT IS ALREADY KNOWN ON THIS TOPIC

⇒ Clinical evidence indicates that increasing the affinity of the Fc region of monoclonal antibodies for the CD16 receptor on natural killer (NK) cells leads to significantly improved therapeutic outcomes.

## WHAT THIS STUDY ADDS

⇒ This study demonstrates the ability of our engineered bispecific immune cell engager with high affinity and specificity for CD16 receptor to activate NK cells and macrophages to kill cancer cells, and effectively eradicate HER2<sup>+</sup> ovarian cancer metastasis in NK humanized hIL15 and hIL-2 NOG mice.

## HOW THIS STUDY MIGHT AFFECT RESEARCH, PRACTICE OR POLICY

⇒ These findings could pave the way for the development of a new generation of potent antibodies for immunotherapy of cancer.

**Conclusions** Collectively, our in vivo findings underscore BiKE:E5C1's potential as an immune cell engager capable of activating immune cells for cancer cell elimination, thereby expanding the arsenal of available BiKEs for cancer immunotherapy.

## BACKGROUND

Antibody-mediated cancer immunotherapy is a type of treatment that uses antibodies to assist the immune system in fighting cancer. The Fab region of monoclonal antibodies (mAbs) binds to antigens on the surface of cancer cells, while their Fc region binds to the Fc receptor CD16a (FcγRIIIA) on natural killer (NK) cells, triggering antibody-dependent cell-mediated cellular cytotoxicity (ADCC).<sup>1</sup> The binding of the Fab region to antigens is typically of high affinity and specificity. However, the Fc region has 'low affinity and specificity' for CD16a.<sup>2,3</sup> This

low-affinity and low-specificity interaction is responsible for the suppressed efficacy of mAbs in cancer therapy,<sup>4-6</sup> as the Fc region also binds to CD32b (FcγRIIB) inhibitory receptor on B cells, macrophages, and a subset of CD8<sup>+</sup> T cells, resulting in the inhibition of B cell maturation, inactivation of macrophages, and reduced T cell survival.<sup>7-9</sup> Consequently, antibody engineers are striving to create antibodies that bind to CD16a with high affinity and specificity, without cross-reactivity with the CD32b receptor.

Our laboratory has successfully isolated and reported the sequence of a single-domain antibody (VHH clone C1) with high affinity and specificity toward CD16a activating receptor, without cross-reactivity with the CD32b inhibitory receptor.<sup>10-11</sup> To assess the potential of VHH clone C1 for activating NK cells and killing cancer cells, we recombinantly fused with an anti-HER2 VHH (clone E5) to create a bispecific killer cell engager (BiKE) (referred to as BiKE:E5C1).<sup>10-12</sup> We have demonstrated that BiKE:E5C1 degranulates and activates NK cells, leading to the release of granzyme B, perforin, TNF- $\alpha$ , and IFN- $\gamma$  at substantially higher levels than Trazimera (trastuzumab), which is considered the best-in-class anti-HER2 mAb currently in clinical use.

To advance our BiKE technology toward clinical application, the objective of this research was to demonstrate the ability of BiKE:E5C1 to activate CD16+ immune cells such as NK cells and macrophages to kill cancer cells in vitro, and eradicate metastatic HER2+ tumors in NK humanized NOG mice. To achieve this objective, HER2+SKOV-3 ovarian cancer cells were injected intraperitoneally (IP) into mice to model metastatic ovarian cancer. Our group and others have shown that NK cells have difficulty recognizing and killing SKOV-3 cells because these cells have low expression levels of MICA/B ligands.<sup>10-13</sup> Hence, this cell line can represent HER2+ cancers that survived NK cell immune surveillance. As effector cells, NK92 cells, which are FDA (Food and Drug Administration) approved for human use and show a broad range of cytotoxicities against cancer cells were used.<sup>14-15</sup> In our in vitro studies, we show that BiKE:E5C1 can activate CD16+ immune cells such as NK cells from peripheral blood (PB-NKs), laNK92 cells, and M1 macrophages to kill cancer cells. In in vivo studies, we employed CD16+laNK92 cells because they could be genetically engineered to express the nanoluciferase gene, making it possible to validate their viability and proliferation using quantitative bioluminescent imaging (qBLI). Since NK92 cells require human interleukin-2 (hIL-2) or human interleukin-15 (hIL-15) to remain viable and active, we evaluated the anticancer efficacy of BiKE:E5C1 in both tumor-bearing NK humanized hIL-15 NOG and hIL-2 NOG mice.

## MATERIALS AND METHODS

### Cell lines and culture

PB-NK cells, SKOV-3 cells, BT-474, and MDA-MB-231 cells were purchased and cultured following vendors' protocols. JIMT-1 (PDX model) HER2<sup>+</sup> breast cancer

cell line resistant to trastuzumab<sup>16</sup> was kindly provided by Dr. Jason S. Lewis (MSKCC, New York, USA). OVASC-1 cells (PDX model), primary cells isolated from ascitic fluid of a patient with advanced drug-resistant epithelial ovarian cancer, were obtained from the Rutgers-Cancer Institute of New Jersey Biorepository center.<sup>17-18</sup> laNK92 cells expressing the low affinity CD16 receptor (F176) were purchased from ATCC (Cat# PTA-8837) in 2019 and cultured as previously described.<sup>10</sup> Currently, laNK92 cell line is not available at ATCC and can be obtained directly from Brink Biologics through an MTA. THP-1-CD16A monocytes stably overexpressing CD16A were generously provided by Dr. Alan H. Lazarus' research group at the University of Toronto.<sup>19</sup> For cell culture details, please see online supplemental method 1.

### Expression and purification of BiKE:E5C1

BiKE:E5C1 was genetically engineered as described previously,<sup>10</sup> cloned into a pET28a vector, transformed into SHuffle *Escherichia coli* expression system, expressed, and then purified using Ni-NTA column chromatography. For details, please see online supplemental method 2.

### Measurement of BiKE-induced ADCC in HER2+ cancer cells using CD16+ immune cells

The ability of BiKE:E5C1 to activate CD16+ immune cells to kill HER2+ cancer cells was measured by ADCC/antibody-dependent cell-mediated phagocytosis (ADCP) assays.

In ADCC assay using CD16+PB-NK or laNK92 cells, SKOV-3 cancer cells were seeded at the density of 10<sup>4</sup> cells per well in a 96-well plate. laNK92 or PB-NK cells were mixed with BiKE:E5C1 (100 nM) and added to the target cells to establish different effector-to-target (E:T) ratios. Cells were then incubated for 24 hours at 37°C. Next, cells were washed with DPBS twice to remove the NK cells from the wells. To evaluate cell viability, alamarBlue HS Cell Viability Reagent was added to the plate and the plate was read using Tecan Infinite M Plex plate reader.

In ADCC assay for measuring the HER2 expression threshold for BiKE:E5C1 activity, CD16+laNK92 cells were used as effector cells, and MDA-MB-231, OVASC-1, JIMT-1, BT-474, and SKOV-3 cells were used as target cells. Cancer cells were seeded in a 96-well plate as mentioned above. laNK92 cells were mixed with BiKE:E5C1 (10 pM), added to target cells to establish different E:T ratios, and then incubated for 6 hours at 37°C. The cancer cell viability was measured as described above.

To assess the potential adverse impact of the IgG<sub>1</sub> Fc region on the anticancer activity of BiKE:E5C1, we conducted a competition ADCC assay. In this experiment, SKOV-3 cells were seeded as mentioned above. Subsequently, laNK92 cells were incubated with a 100 nM concentration of the 3G8 anti-CD16 antibody for 30 min in the incubator. Concurrently, 1 nM of either BiKE:E5C1 or trastuzumab was added to the SKOV-3 cells and incubated for 30 min in the incubator. Following this, laNK92 cells were added to the SKOV-3 cells at an ET ratio of

4, and the ADCC assay was performed for a duration of 4 hours. Postassay, a thorough washing step was carried out to eliminate floating cells, and alamar Blue was employed to evaluate cell viability.

In ADCP assay using THP-1-CD16A cells, first the expression levels of CD16a on the surface of monocytes was measured using flow cytometry and 3G8 anti-CD16 mAb (Thermo Fisher, Cat#MHCD1605). Then THP-1-CD16A monocytes were seeded at the density of  $2 \times 10^4$  cells per well in a 96-well plate and treated with 100 ng/mL of Phorbol-12-Myristate-13-Acetate to polarize the cells into M0 THP-1-CD16A macrophages. Cells were incubated under this condition at 37°C for 24 hours. Subsequently, the M0 macrophages were treated with 100 ng/mL lipopolysaccharide (LPS) (Millipore Sigma, Cat#L2630-10MG) and 20 ng/mL of IFN- $\gamma$  (Peprotech, Cat#300-02-100UG) and incubated at 37°C for 24 hours to transform them into M1 macrophage. Then, the expression of CD80 (M1 macrophage biomarker)<sup>20</sup> was measured using flow cytometry and anti-CD80 mAb (Biolegend, Cat# 305219). To measure ADCP, THP-1-CD16A cells were seeded at the density of  $2 \times 10^4$  cells per well in a 96-well plate and then differentiated into M1 macrophages as mentioned above. Subsequently, firefly luciferase-expressing SKOV-3 cells were opsonized with an equimolar quantity of either BiKE:E5C1 or trastuzumab (positive control). Following opsonization, 4000 SKOV-3 cells were added to the M1 macrophages achieving an E:T ratio of 5. Cells were coincubated for 24 hours at 37°C. The next day, cells were washed with DPBS twice, and then the bioluminescence of viable cells were measured using the Promega Luciferase Assay kit.

#### Measurement of the degranulation of laNK92 cells using surfaced CD107a

To measure degranulation of laNK92 cells, surfaced CD107a was measured following a previously published method.<sup>10</sup> For more details, please see online supplemental method 3.

#### Evaluation of the impact of hIL-2 and hIL-15 on laNK92 cytotoxicity

To assess the impact of hIL-2 and hIL-15 on the cytotoxicity of laNK92 cells, we conducted an ADCC assay employing various BiKE:E5C1 concentrations while maintaining a constant E:T ratio of 4, as well as different E:T ratios while maintaining a fixed BiKE:E5C1 concentration (100 nM). For more details, please see online supplemental method 4.

#### Quantification of cytokine release

To measure the amounts of TNF- $\alpha$  and IFN- $\gamma$  released from the activated NK cells, an ELISA was performed. For details, please see online supplemental method 5.

#### Generation and characterization of nanoluciferase-expressing laNK92 stable cell line

The gene encoding nanoluciferase (NanoLuc, Promega, Madison, Wisconsin USA) was designed under an EF1- $\alpha$

promoter, synthesized by VectorBuilder (Santa Clara, California, USA), and then cloned into a mammalian cell expression PiggyBac vector (pb-nLuc). For details, please see online supplemental method 6.

#### Evaluation of the viability of laNK92 cells in hIL-15 NOG and hIL-2 NOG mice

We also used the ARRIVE reporting guidelines.<sup>21</sup> First, mice were preconditioned by one time IP injection of 20 mg/kg of busulfan (Millipore Sigma, B2635-25G).<sup>22</sup> The next day, 2M laNK92-nLuc cells were injected IP into female hIL-2 NOG aged 4–6 weeks (model# 13440-F), hIL-15 NOG (model# 13683-F), and CIEA NOG (model# NOG-F) mice (Taconic Biosciences). One CIEA NOG mouse received daily injection of hIL-2 (50K UI) for five consecutive days, whereas the second one did not receive any hIL-2. Before imaging, mice were anesthetized by 2% isoflurane and then injected IP with furimazine (Promega) (2  $\mu$ L furimazine in 198  $\mu$ L of DPBS). The BLI in each mouse was detected within 30 s of furimazine injection with acquisition time of 60 s using an IVIS Lumina III Imaging System. To determine the fold change in mass of laNK92-nLuc cells over time, the total BLI of the mouse body on day 35 was divided by the total BLI of the same mouse on day 1.

#### Evaluation of the ability of BiKE:E5C1 to activate laNK92 cells to kill SKOV-3 tumors in mice

hIL-2 NOG and hIL-15 NOG mice were preconditioned with Busulfan as mentioned above. The next day,  $1 \times 10^6$  firefly luciferase-expressing SKOV-3 cells were injected IP into mice to induce intraperitoneal tumors. After 3 days, D-luciferin substrate was injected IP to image and verify the establishment of the tumors. Next, tumor-bearing mice were divided into three groups of six mice. One group received BiKE:E5C1 only (200  $\mu$ g/mouse), the second group received laNK92-nLuc cells only (4 million/mouse), and the third group received laNK92-nLuc cells (4 million/mouse) plus BiKE:E5C1 (200  $\mu$ g/mouse). laNK92-nLuc cells were injected IP once. BiKE:E5C1 was administered IP daily, five times a week, and for 2–3 weeks. The viability of laNK92-nLuc cells was monitored weekly using furimazine (nLuc substrate). The response to therapy was evaluated by injecting 150 mg/kg of D-luciferin (fLuc substrate) (GoldBio, Missouri, USA) dissolved in 200  $\mu$ L of DPBS and measuring the BLI of tumors over time. Mice were imaged within 10 min of D-luciferin injection with acquisition times of 60 s using an IVIS Lumina III Imaging System and analyzed. The fLuc substrate (D-luciferin) and nLuc substrate (furimazine) are enzyme specific and do not cross react. To determine the fold change in mass of SKOV-3 cells over time, the total BLI of the mouse body on the last time point was divided by the total BLI of the same mouse on the first point. Observable indicators of health (ie, diarrhea, appetite, posture, and movement) and body weight were continuously monitored to detect any treatment-related toxicities. Loss of more than 10% body weight in



1 week or more than 20% at any time was considered as the study endpoint.

## RESULTS

### BiKE:E5C1 helps CD16+ PB-NK cells, laNK92 cells, and THP-1-CD16A macrophages kill cancer cells

The aim of this experiment was to demonstrate the capacity of BiKE:E5C1 to engage CD16-expressing immune cells and enhance their effectiveness in killing cancer cells. To achieve this goal, three different types of CD16-expressing immune cells were used: PB-NK cells, laNK92 cells, and THP-1-CD16A monocytes.

First, we investigated the ability of BiKE:E5C1 to engage and enhance the efficacy of PB-NK cells in killing HER2+ cancer cells. In this context, CD16+PB-NK cells were cocultured with HER2+SKOV-3 ovarian cancer cells in the presence of BiKE:E5C1. The expression of CD16 receptor

on PB-NK cells was confirmed by flow cytometry (online supplemental figure 1). The results of the ADCC assay demonstrated a significant enhancement in the killing efficiency of PB-NK cells against SKOV-3 cells when combined with BiKE:E5C1 (figure 1A). Analysis of ELISA data revealed a substantial increase in the quantities of TNF- $\alpha$  and IFN- $\gamma$  released by PB-NK cells in the presence of BiKE:E5C1 (figure 1B,C).

For comparison purposes, we conducted an ADCC assay using laNK92 cells. In this experiment, CD16+laNK92 cells were cocultured with SKOV-3 cells in the presence or absence of BiKE:E5C1. The results indicated that BiKE:E5C1 significantly enhanced the cytotoxicity of laNK92 against SKOV-3 cancer cells at all E:T ratios, similar to PB-NK cells (figure 1D). As we have previously demonstrated, BiKE:E5C1 can engage the CD16a receptor on laNK92 cells, activating them to release

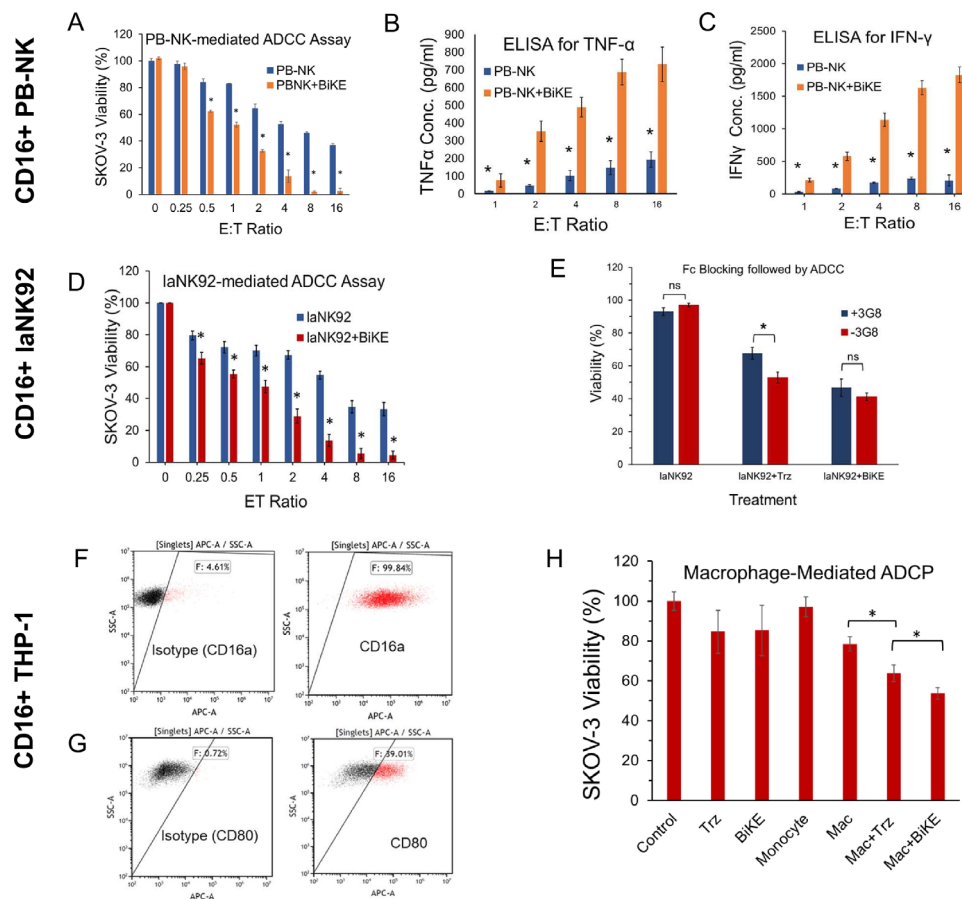


**Figure 1** Evaluation of CD16a+ immune cell activation by BiKE:E5C1. (A–C) Activation of PB-NK cells by BiKE:E5C1, resulting in a significant increase in cytokine release and the death of HER2+SKOV-3 cancer cells. (D) ADCC assay demonstrating BiKE:E5C1's capacity to enhance the cancer-killing efficiency of laNK92 cells. (E) ADCC assay conducted in the presence and absence of 3G8 anti-CD16 antibody. This figure highlights that the anticancer activity of BiKE:E5C1 remains unaffected by IgG<sub>1</sub> Fc region, while 3G8 significantly reduces the efficacy of trastuzumab (IgG<sub>1</sub>-based mAb). (F–G) Flow cytometry analysis of surface biomarkers, CD16a on THP-1-CD16A monocytes and CD80 on M1 macrophages. (H) ADCP assay demonstrating BiKE:E5C1's potential to enhance the anticancer activity of M1 macrophages. The following groups are shown: control (SKOV-3 alone untreated), Trz (SKOV-3 treated with trastuzumab), BiKE (SKOV-3 treated with BiKE), monocyte (SKOV-3 treated with THP-1-CD16A monocytes), Mac (SKOV-3 treated with M1 THP-1-CD16A macrophages), Mac+Trz (SKOV-3 treated with M1 THP-1-CD16A macrophages plus trastuzumab), and Mac+BiKE (SKOV-3 treated with M1 THP-1-CD16A macrophages plus BiKE). Data are presented as mean $\pm$ SD. (n=5); \*t-test, p<0.05. ADCC, antibody-dependent cell-mediated cytotoxicity; BiKE, bispecific killer cell engager; NK, natural killer; ns, not significant; PB, peripheral blood.

substantial amounts of perforin, granzyme B, TNF- $\alpha$ , and IFN- $\gamma$ , ultimately leading to the killing of HER2+ cancer cells.<sup>10</sup>

Subsequently, we examined whether IgG<sub>1</sub> Fc region could compete with BiKE:E5C1 for binding to the CD16a receptor, potentially reducing its activity. An anti-CD16 mAb (ie, 3G8) that targets the same epitope on CD16a receptor as IgG<sub>1</sub> Fc was used as a competitor.<sup>23</sup> Trastuzumab, an IgG<sub>1</sub>-based mAb, was used as a control. The ADCC assay results indicated that the presence of 3G8 had no significant impact on the anticancer efficacy of BiKE:E5C1. However, 3G8 mAb significantly reduced the efficacy of trastuzumab (figure 1E). As BiKE:E5C1 recognizes a different epitope on CD16a than IgG<sub>1</sub>,<sup>10</sup> its anticancer activity remained unaffected.

Furthermore, the ability of THP-1-CD16a monocyte-macrophages to engulf (phagocytose) antibody-opsonized human red blood cells and platelets had previously been demonstrated using ADCP assay.<sup>24</sup> Employing ADCP assay, we explored the potential of BiKE:E5C1 to enhance the anticancer activity of CD16+M1 macrophages (downstream effect) against SKOV-3 cells. To achieve this, THP-1-CD16a monocytes that were engineered to stably express CD16a receptor (figure 1F), were treated with LPS and IFN- $\gamma$  to polarize them into M1 macrophages. The results of this experiment revealed that approximately 40% of the THP-1-CD16a monocytes were successfully polarized into M1 macrophages as indicated by the expression of the CD80 antigen (figure 1G). These macrophages were then coincubated with SKOV-3 cells in the presence of BiKE:E5C1. The results of the ADCP assay showed that BiKE:E5C1 could enhance the killing efficiency of macrophages more significantly than trastuzumab (figure 1H).

### BiKE can activate laNK92 cells to kill cancer cells with a wide range of HER2 expression levels

In immunohistochemistry (IHC) analysis, tumor tissues are scored as 0, 1+, 2+, and 3+. Scores of 0 and 1 are considered HER2-, even though HER2 is slightly present. A score of 2 is considered equivocal, and a

score of 3 means HER2+ status.<sup>12 25</sup> To determine the threshold of HER2 expression level that would make BiKE:E5C1 functional, first a panel of HER2-expressing cancer cells was carefully selected and analyzed by flow cytometry. The results of this experiment showed that MDA-MB-231 cells (HER2-, IHC score 0) had the lowest expression of HER2, and SKOV-3 cells had the highest (HER2+, IHC score 3+) (figure 2A,B). Next, the ability of laNK92 cells to kill the aforementioned cancer cells in the presence of BiKE:E5C1 (10 pM) was measured. The results of the ADCC assay revealed that the viability of MDA-MB-231 cells was not significantly affected by BiKE:E5C1 plus laNK92 cells; however, all other cancer cells that had expression of HER2 ranging from low to high were responsive to therapy (figure 2C). Interestingly, low HER2-expressing OVASC-1 cells (75% positive with low MFI) and trastuzumab-resistant JIMT-1 cells (HER2+) could be targeted and killed. hIL-2 and hIL-15 have similar effects on killing efficiency of laNK92 cells.

NK92 is an immortalized human NK cell line that requires hIL-2 for both its proliferation and activity.<sup>26 27</sup> However, a recent study has reported that NK92 cells can sustain their proliferation and activity not only in the presence of hIL-2 but also hIL-15 (equal amounts).<sup>28</sup> To assess the impact of these two cytokines on the cytotoxicity of NK92 cells, we cultured them in the presence of each cytokine for 2 weeks at equimolar doses and subsequently evaluated their anticancer activity against SKOV-3 cells. The results of the ADCC assay revealed there was no statistically significant difference between the cytotoxicities of the laNK92 cells cultured under these conditions (figure 3A,B). Measurement of the laNK92 cell degranulation, CD16 expression levels, and the secretion of TNF- $\alpha$  and IFN- $\gamma$  after activation with BiKE:E5C1 also demonstrated a similar level of NK cell activation (figure 3C-G).

### Genetic engineering of luciferase-expressing laNK92-nLuc cells

To facilitate the monitoring of the viability and proliferation of laNK92 cells in mice, they were genetically engineered

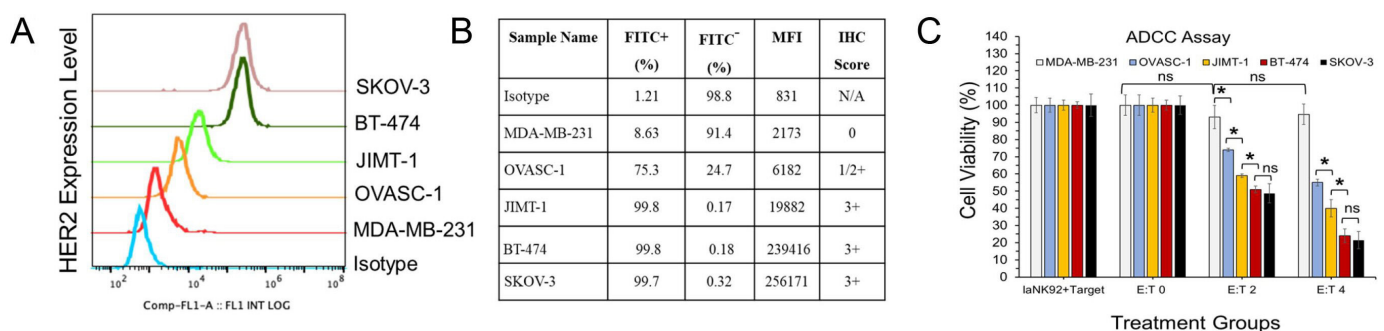


**Figure 2** (A, B) Measurement of the HER2 expression on the surface of cancer cells using anti-HER2 antibody (trastuzumab) and flow cytometry. The percentages of the cells that were labeled with fluorescein (FITC) dye, mean fluorescent intensity (MFI) of labeled cells, and IHC scores of each cell line are also shown. (C) ADCC assay using BiKE:E5C1 at 10 pM concentration and laNK92 at different E:T ratios. E:T 0 corresponds to target+BiKE treatment group (no laNK92). Data are normalized against laNK92+target group and presented as mean $\pm$ SD. (n=3). \*p<0.05. ADCC, antibody-dependent cell-mediated cytotoxicity; BiKE, bispecific killer cell engager; E:T, effector-to-target; ns, not significant.

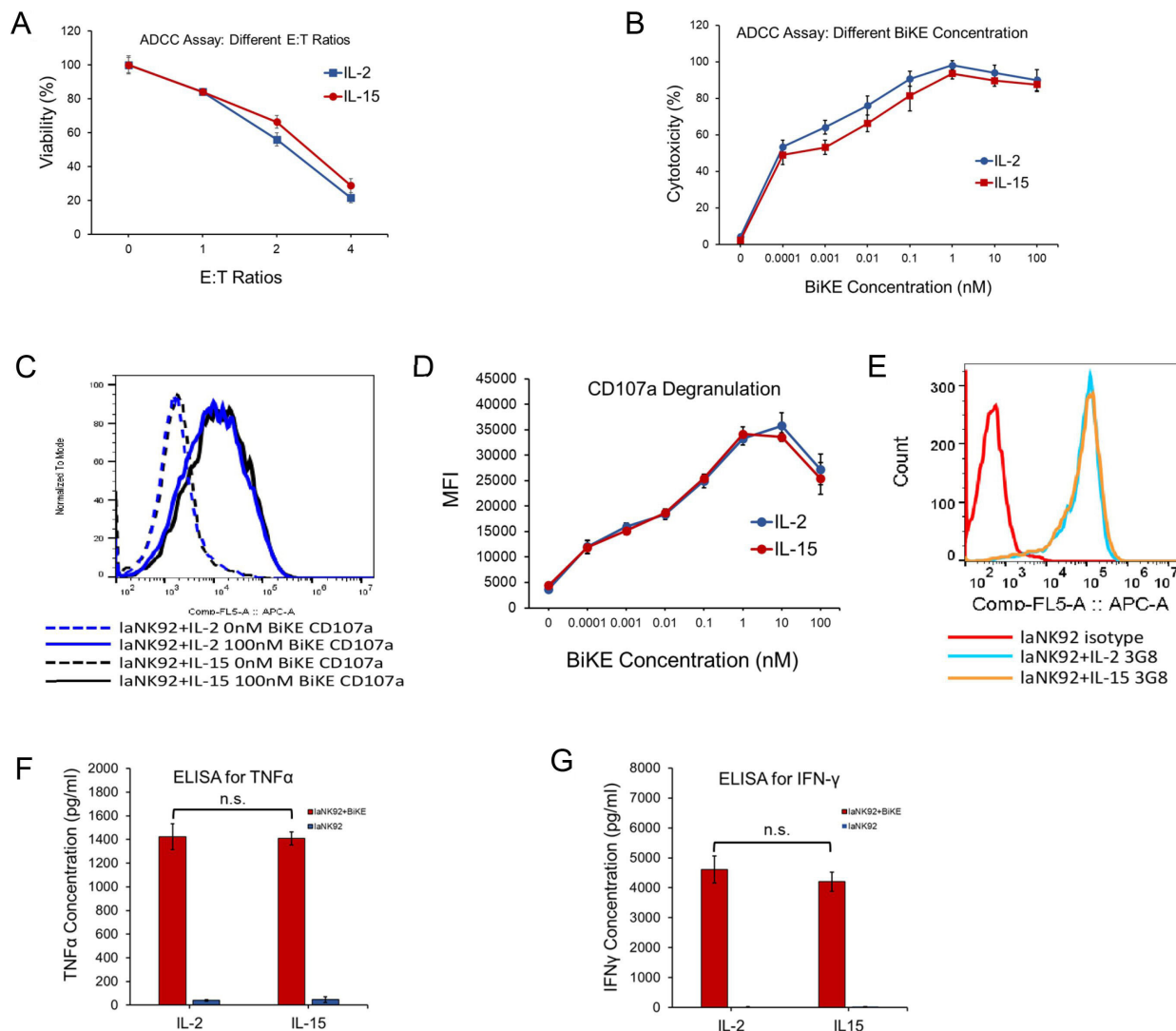


**Figure 3** Evaluation of the impact on IL-2 and IL-15 on the cytotoxicity, CD16 expression levels, degranulation, and activation of laNK92 cells. (A) Measurement of the cytotoxicity of BiKE:E5C1 plus laNK92 cells at different E:T ratios on SKOV-3 cells using ADCC assay. (B) Measurement of the cytotoxicity of BiKE:E5C1 plus laNK92 cells at different concentrations (E:T ratio of 4) on SKOV-3 cells using ADCC assay. (C, D) Measurement of the degranulation of laNK92 cells after activation with BiKE:E5C1 and incubation with SKOV-3 cells. (E) Measurement of the expression levels of CD16 receptor on laNK92 cells cultured in the presence of hIL-2 or hIL-15 using 3G8 anti-CD16 antibody. (F, G) Quantification of TNF- $\alpha$  and IFN- $\gamma$  released from the laNK92 cells conditioned in hIL-2 or hIL-15 before and after activation by BiKE:E5C1. Data are presented as mean $\pm$ SD. (n=4). ADCC, antibody-dependent cell-mediated cytotoxicity; BiKE, bispecific killer cell engager; E:T, effector-to-target; ns, not significant; MFI, mean fluorescent intensity.

to stably express nanoluciferase gene (laNK92-nLuc). To examine whether the genetic modification procedure affected the expression levels of CD16a receptor, proliferation rate, and killing efficiency of laNK92 cells, we employed flow cytometry and ADCC assays. The flow cytometry data indicated that there was no significant difference between the percentages of CD16a-expressing cells in laNK92 and laNK92-nLuc populations; however, the density of CD16a receptor on laNK92-nLuc cells was approximately 20% higher than on parent laNK92 cells (figure 4A,B). We also observed that the proliferation rate of laNK92-nLuc cells was somewhat higher (~10%) than that of parent laNK92 cells (figure 4C,D). Nevertheless, the results of the ADCC assay, conducted at different

E:T ratios and antibody concentrations, showed that there was no significant difference between the engineered laNK92-nLuc cells and the parent cell population (figure 4E,F).

#### hIL-2 NOG and hIL-15 NOG mice support the proliferation of NK92 cells

The objective of this experiment was to assess whether the concentrations of hIL-2 in hIL-2 NOG and hIL-15 in hIL-15 NOG mice were adequate to sustain the viability and proliferation of laNK92 cells. It is noteworthy that the reported concentration of hIL-2 in the plasma of hIL-2 NOG mice ranges from 1 to 3 ng/mL, while the concentration of hIL-15 in the plasma of hIL-15 NOG

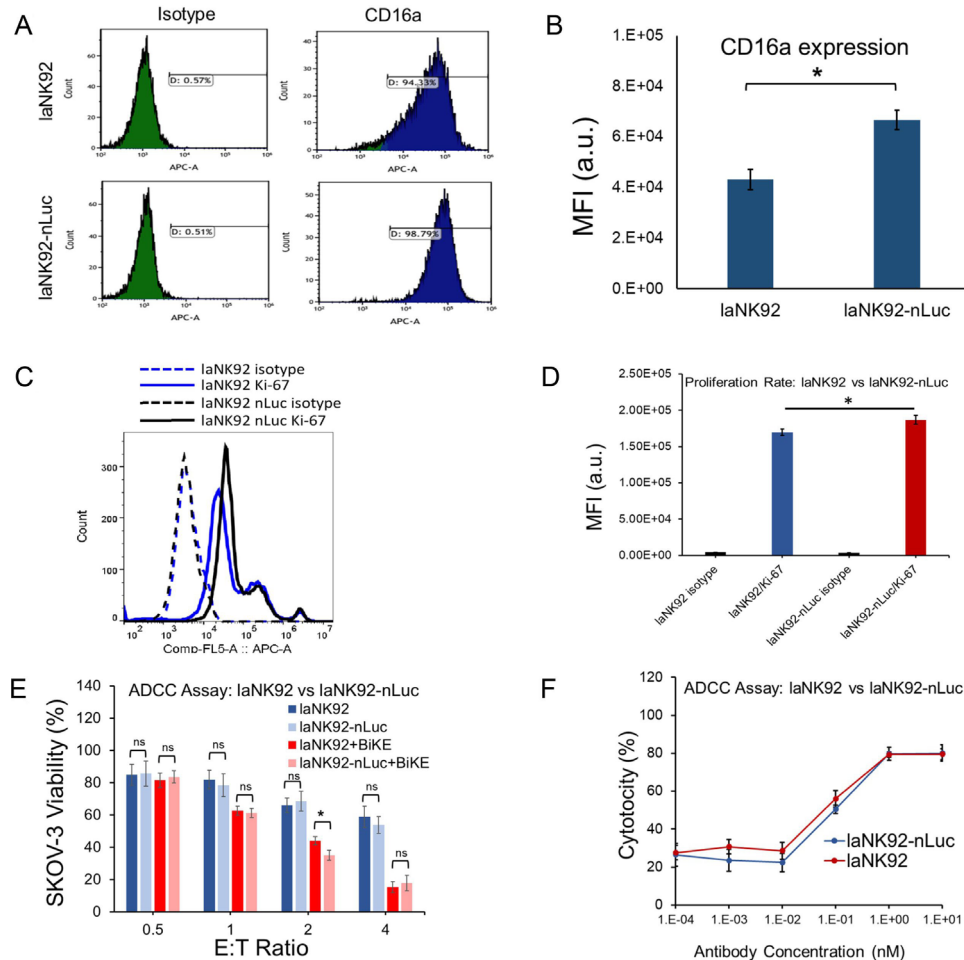


**Figure 4** Characterization of laNK92-nLuc cells. (A, B) Measurement of the expression levels of CD16a receptor on the surfaces of laNK92 and laNK92-nLuc cells using flow cytometry. (C, D) Measurement of the proliferation rates of laNK92 and laNK92-nLuc cells using flow cytometry. (E, F) Measurement of the killing efficiencies of laNK92 and laNK92-nLuc cells at different E:T ratios and antibody concentrations using ADCC assay. Data are presented as mean $\pm$ SD. (n=3); \*t-test,  $p < 0.05$ . ADCC, antibody-dependent cell-mediated cytotoxicity; BiKE, bispecific killer cell engager; E:T, effector-to-target; ns, not significant.

mice is documented as 50 pg/mL,<sup>29 30</sup> indicating a 20–50 fold difference in cytokine concentrations between the two models. However, internal data from Taconic Biosciences, as measured by serology testing, indicate that the concentrations of hIL-2 and hIL-15 in the mentioned models are in the range of 0.5–2.0 ng/mL and 1–4 ng/mL, respectively. To investigate further, laNK92-nLuc cells were injected IP into hIL-2 NOG and hIL-15 NOG mice, while CIEA NOG mice, which do not express hIL-2 or hIL-15 served as controls. The results of this experiment demonstrated that laNK92-nLuc cells remained viable and proliferated in both hIL-2 NOG and hIL-15 NOG mice (figure 5A–F). As expected, laNK92-nLuc cells were unable to maintain viability in CIEA NOG mice (figure 5G,H). Statistical analysis of data showed that there was no significant difference between the growth rates of laNK92-nLuc cells in hIL-2 NOG and hIL-15 NOG mice (t-test, \* $p < 0.05$ ) (figure 5I). We also observed that the mice in the hIL-2 NOG group showed signs of toxicity, such as lethargy, loss of appetite, and reduced activity, more significantly and 1 week earlier than those

in hIL-15 NOG group. All mice showed signs of toxicity ~30 days post-NK cell injection and died approximately after 40 days.

#### laNK92 cells in combination with BiKE:E5C1 eliminate HER2+ tumors in hIL-15 NOG mice

The aim of this experiment was to demonstrate the functionality of the BiKE:E5C1 under in vivo conditions and validate the in vitro data. To achieve this goal, SKOV-3 tumors were implanted IP in hIL-15 NOG mice and then treated with laNK92-nLuc alone, BiKE:E5C1 alone, or laNK92-nLuc plus BiKE:E5C1 following the dosing schedule shown in figure 6A. The results of this study showed that the tumor-bearing mice treated with laNK92-nLuc plus BiKE:E5C1 fully responded to the therapy, and bioluminescence of cancer cells was not detectable after 2 weeks (figure 6B,C). In contrast, mice treated with laNK92-nLuc or BiKE:E5C1 alone did not respond to therapy and there was no significant reduction in tumor mass over time (figure 6E–I). Measurement of body weight during the treatment period showed that all



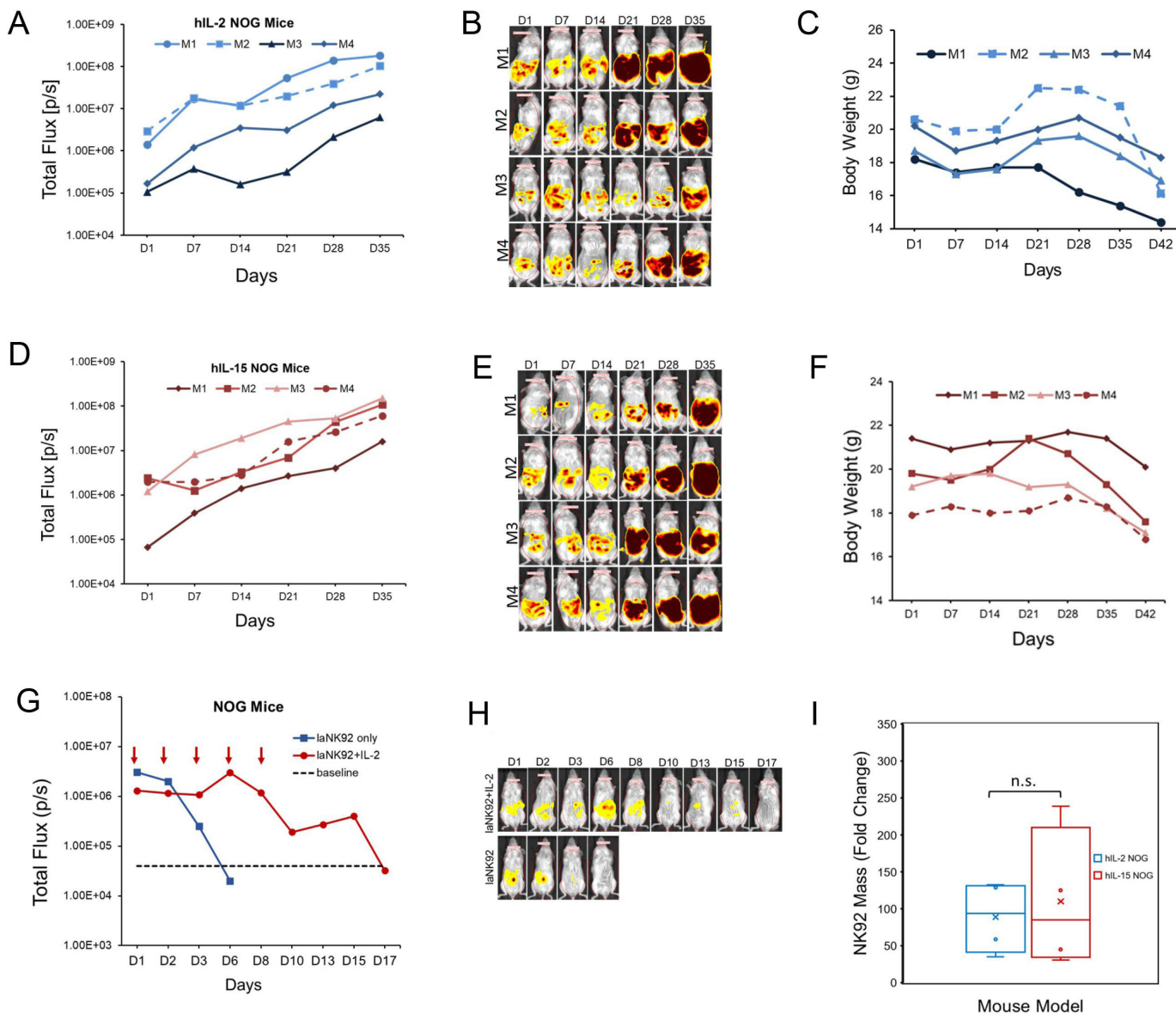


**Figure 5** Evaluation of the viability and proliferation of laNK92-nLuc cells in NOG mice. (A–C) Measurement of the BLI of laNK92-nLuc cells over time and hIL-2 NOG mouse body weights after IP injections. (D–F) Measurement of the BLI of laNK92-nLuc cells over time and hIL-15 NOG mouse body weights after IP injections. (G, H) Measurement of the BLI of laNK92-nLuc cells in CIEA NOG mice in the presence and absence of hIL-2 injections. (I) Statistical analysis of changes in laNK92-nLuc mass in hIL-2 NOG and hIL-15 NOG mice over the 35-day period. Data are presented as mean $\pm$ SD. (n=4). BLI, bioluminescent imaging; IP, intraperitoneally; ns, not significant.

mice maintained their weights without any significant loss (figure 6D, G and J). Analysis of data showed a statistically significant difference between the test and control groups (analysis of variance followed by post hoc Tukey test, \* $p < 0.05$ ) (figure 6K). As an indication of the killer cell engagement of laNK92-nLuc cells in the presence of BiKE:E5C1, we also measured the concentration of IFN- $\gamma$  in mice blood. The results of this assay showed a significant increase in the concentration of IFN- $\gamma$  in the blood of mice that were treated with laNK92-nLuc cells plus BiKE:E5C1, indicating activation of laNK92-nLuc cells (figure 6L). It is also noteworthy that BiKE:E5C1 does not have any cross-reactivity with mice CD16 antigens; thereby limiting its interactions to CD16a on laNK92 cells only

(online supplemental figure 2). Measurement of the BLI (nLuc) for laNK92 cells confirmed that they remained viable over the treatment period (figure 6M–P).

#### laNK92 cells in combination with BiKE:E5C1 eliminate HER2+ tumors in hIL-2 NOG mice

To demonstrate that BiKE:E5C1's efficacy is not limited to hIL-15 NOG mice, we implanted SKOV-3 tumors into the peritoneal cavity of hIL-2 NOG mice, following the same procedure mentioned above, and subsequently treated them with laNK92-nLuc plus BiKE:E5C1 using the identical treatment protocol (figure 6A). A second group of tumor-bearing hIL-2 NOG mice received treatment with laNK92-nLuc cells alone and was used as a



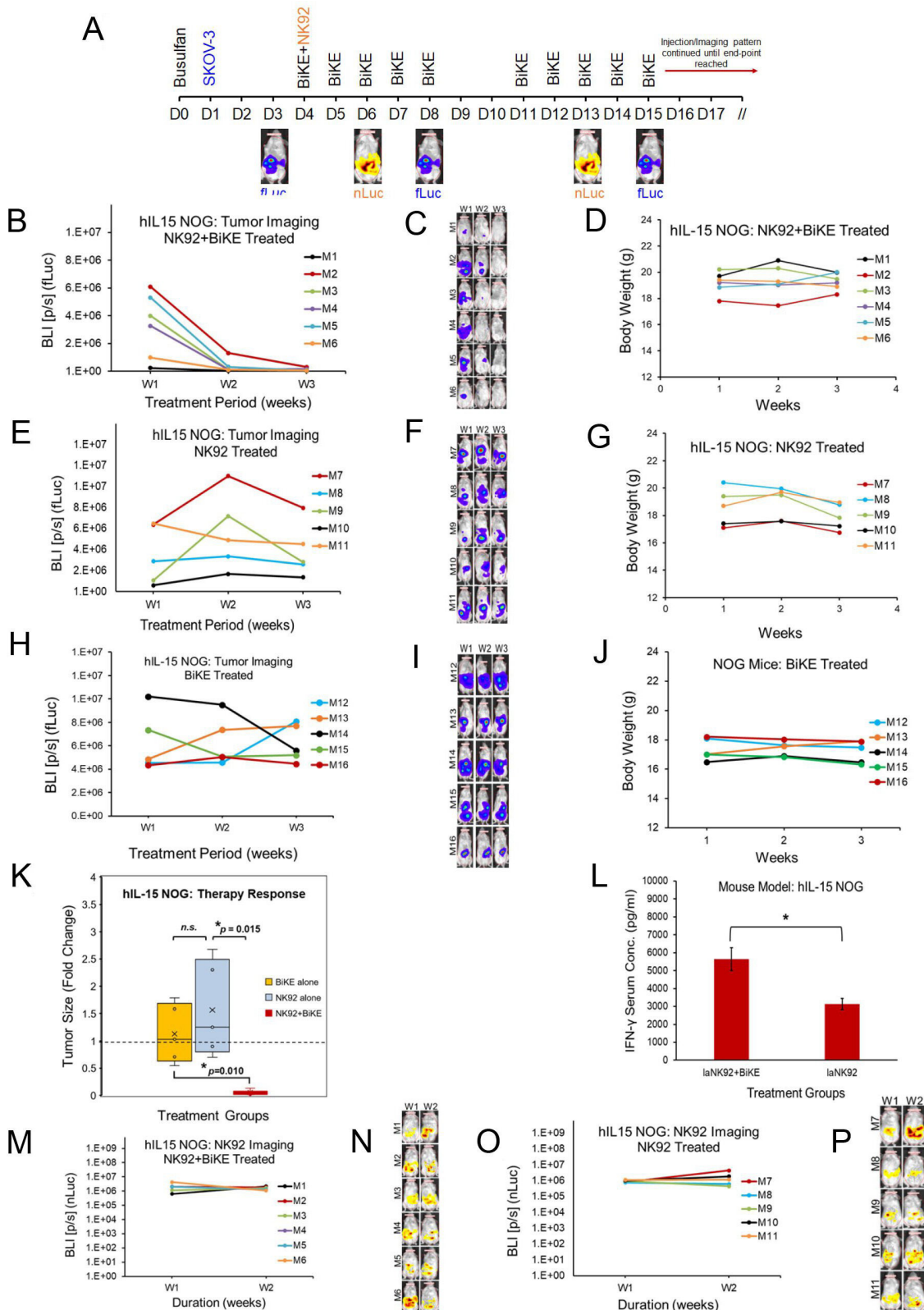


**Figure 6** Evaluation of the ability of BiKE:E5C1 to activate laNK92-nLuc cells to kill HER2+ cancer cells in hIL-15 NOG mice. (A) The dosing schedule used to implant SKOV-3 cells in mice followed by one time injection of laNK92-nLuc cells and daily injection of BiKE:E5C1. (B–J) Measurement of the BLI of tumor mass over time and body weight of hIL-15 NOG mice that were treated with BiKE:E5C1+laNK92 nLuc cells, laNK92-nLuc cells alone, or BiKE:E5C1 alone. (K) Box-Whisker plot and statistical analysis of change in tumor mass over time in test and control groups. ANOVA followed by post hoc Tukey test, \* $p < 0.05$ . (L) Measurement of IFN- $\gamma$  in the plasma of hIL-15 NOG mice. \* $t$ -test,  $p < 0.05$ . Data are presented as mean  $\pm$  SD. (M–P) BLI (nLuc) of laNK92-nLuc cells in test and control groups validating their viability over the treatment period. ANOVA, analysis of variance; BiKE, bispecific killer cell engager; BLI, bioluminescent imaging.

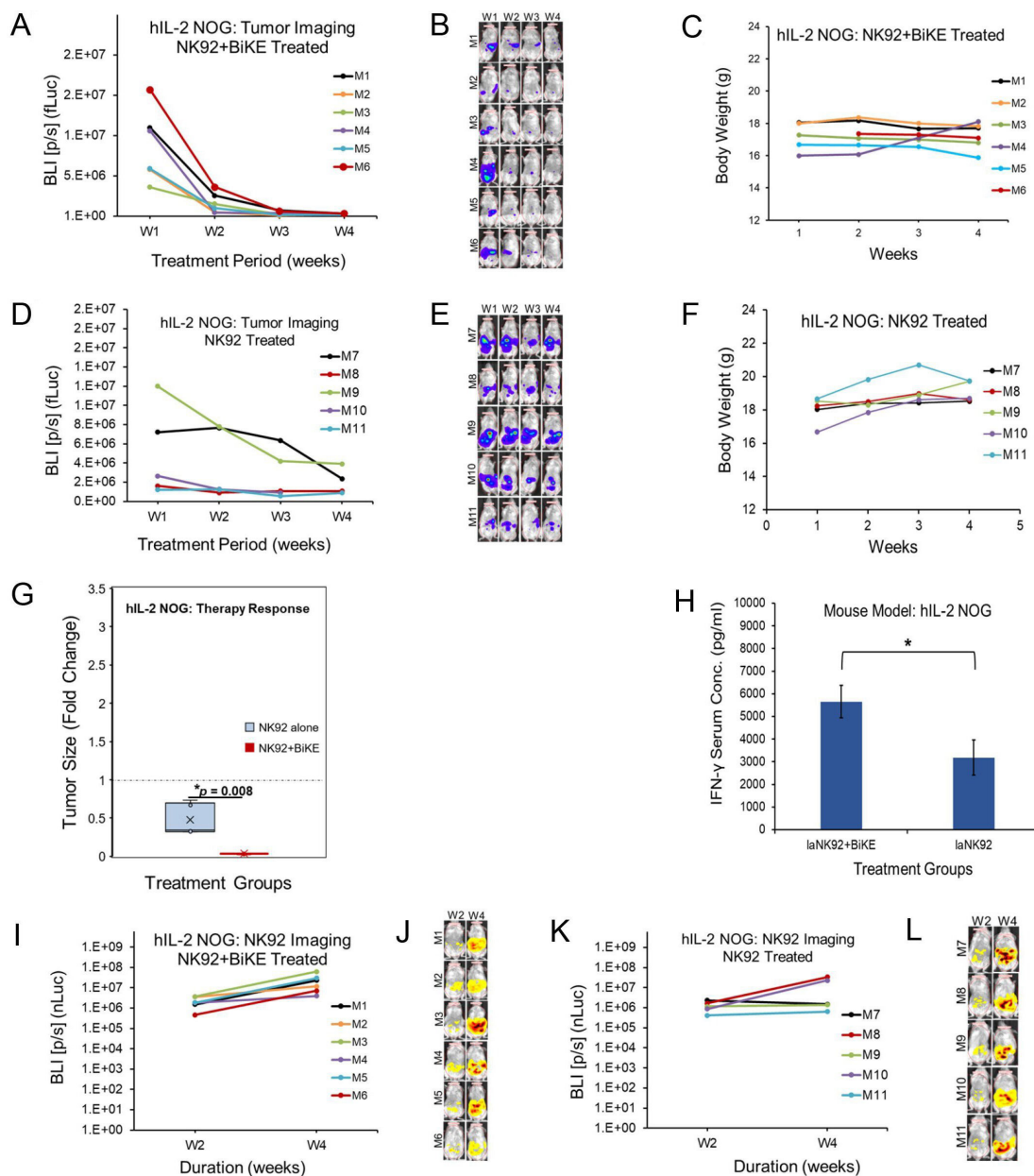


**Figure 7** Evaluation of the ability of BiKE:E5C1 to activate laNK92-nLuc cells to kill HER2+ cancer cells in hIL-2 NOG mice. (A–F) Measurement of the BLI of tumor mass over time and body weight of hIL-2 NOG mice that were treated with BiKE:E5C1+laNK92 nLuc cells or laNK92-nLuc cells alone. (G) Box-Whisker plot and statistical analysis of change in tumor mass over time in test and control group. t-test,  $*p < 0.05$ . (H) Measurement of IFN- $\gamma$  in the plasma of hIL-15 NOG mice. \*t-test,  $p < 0.05$ . Data are presented as mean  $\pm$  SD. (I–L) BLI (nLuc) of laNK92-nLuc cells in test and control groups validating the viability of the cells over the treatment period. BiKE, bispecific killer cell engager.

control. Since we previously established that BiKE:E5C1 alone does not exhibit anticancer activity at the administered dose (figure 6H,K), we did not include this group as a control in this experiment to avoid redundancy. The results of this experiment revealed that BiKE:E5C1 could activate laNK92-nLuc cells in hIL-2 NOG mice to effectively eliminate SKOV-3 cancer cells (figure 7A,B). Although tumor-bearing hIL-2 NOG mice that were treated with laNK92 cells alone responded positively to the therapy (figure 7D,E), analysis of the data showed a statistically significant difference between the test and control group (t-test,  $*p < 0.05$ ) (figure 7G). Measurement

of the concentration of IFN- $\gamma$  in mice serum demonstrated an increase in the concentration of IFN- $\gamma$  in mice that were treated with laNK92-nLuc cells plus BiKE:E5C1, indicating activation of laNK92-nLuc cells by BiKE:E5C1 (figure 7H). Measurement of the BLI (nLuc) for laNK92 cells confirmed that they remained viable over the treatment period (figure 7I–L).

## DISCUSSION

NK cells naturally possess the ability to kill tumor cells without prior sensitization and modulate antitumor

functions via cytokine secretion.<sup>31</sup> Therapeutic mAbs inducing NK cell-mediated ADCC and genetically engineered CAR-NK cells have been developed for cancer treatment. However, these two modalities bear some inherent limitations. For instance, polymorphism of CD16a has been reported to impact human IgG<sub>1</sub> binding and subsequently influence NK cell ADCC.<sup>32</sup> Moreover, it is well understood that CAR-NK cells present significant challenges in genetic manipulation, and their antitumor efficacy is limited by the short life of NK cells.<sup>33</sup> While earlier reports indicated that NK therapy had no significant side effects, such as cytokine release syndrome (CRS), Zhang *et al* recently published clinical data on the use of the third generation of CAR-NK cells (referred to as CCCR-NK92) and observed CRS in one patient.<sup>34</sup> Another class of immunotherapeutic modalities harnessing NK cells, known as NK cell engagers (NKCEs), has recently emerged and exhibited several advantages over the abovementioned strategies.<sup>35</sup>

In this context, we have previously reported the sequence of a new NKCE (BiKE:E5C1) and have shown under *in vitro* conditions that it forms an immunologic synapse between laNK92 cells and HER2+ cancer cells, leading to the lysis of cancer cells.<sup>10</sup> As a first step toward achieving our objective, we evaluated the ability of BiKE:E5C1 to activate other immune cells that express CD16a receptor. Our data showed that BiKE:E5C1 has the ability to activate not only laNK92 cells but also PB-NKs cells and macrophages, significantly enhancing their anticancer activity (figure 1). This indicates that the efficacy of BiKE:E5C1 is not limited to NK cells but can extend to all immune cells that express CD16a receptor on their surfaces. Interestingly, we observed that IgG-based mAbs do not interfere with the activity of BiKE:E5C1, as they recognize different epitopes on CD16a receptors, thereby providing the opportunity for combination therapy with other mAbs. For examples, we have shown that BiKE:E5C1 in combination with pertuzumab has significantly higher anticancer activity than BiKE:E5C1 or pertuzumab alone.<sup>12</sup>

In the next step, we examined the ability of BiKE:E5C1 to activate laNK92 cells and kill cancer cells with a wide range of HER2 expression levels. While BiKE-activated laNK92 cells were unable to kill HER2- MDA-MB-231 cells, they could facilitate the killing of not only OVASC-1 HER2-low cancer cells but also trastuzumab-resistant JIMT-1 cells (figure 2). This suggests that BiKE:E5C1 could potentially compete with current FDA-approved antibody-drug conjugates such as Enhertu for the treatment of cancers in HER2-low category.

Learning that BiKE:E5C1 can activate both PB-NKs and laNK92 cells, we selected laNK92 cells as effector cells for our *in vivo* studies since they are immortalized and come from a single donor, providing a consistent source of NK cells without the difficulties associated with PB-NK cells, such as short lifespan and donor batch-to-batch variations. For this purpose, we first cultured laNK92 cells in the presence of hIL-2 and hIL-15 at equimolar doses to

determine whether they have any impact on their cytotoxicity. We performed this study because Törnroos *et al*, recently reported that treating NK92 cells with hIL-15 enhanced their proliferation rate significantly more than those cultured in the presence of hIL-2.<sup>28</sup> Here, we conducted a comprehensive examination of the impact of hIL-2 and hIL-15 on laNK92-mediated ADCC. Our data show that regardless of the cytokine used, there is no significant difference in killing efficiency, CD16 expression, or cytokine release from laNK92 cells cultured under these two conditions (figure 3). Before initiating *in vivo* experiments, we genetically engineered laNK92-nLuc cells to make it possible for us to monitor their fate (viability and proliferation) after injection into mice. Biological characterization of laNK92-nLuc cells illustrated that, despite a slightly higher proliferation rate for the laNK92-nLuc cells, these cells were in general similar to their parent cells without any significant difference in killing efficiency (figure 4). It is noteworthy that in our ADCC assay, we introduced an equal number of laNK92 and laNK92-nLuc cells to the cancer cells, and the experiments were conducted over a relatively short period of time (ie, 4 hours). This short incubation time eliminated the opportunity for laNK92 cells to undergo substantial expansion affecting the E:T ratios.

As there were no previous reports in the literature regarding the viability of laNK92 cells in NOG mouse models and their potential toxicity to the host, we conducted an experiment in which we injected laNK92-nLuc cells into CIEA NOG, hIL-2 NOG, and hIL-15 NOG mice to determine the most suitable model for *in vivo* BiKE efficacy studies. Our data revealed that CIEA NOG mice did not support the growth of laNK92-nLuc cells. In contrast, both hIL-2 and hIL-15 mice sustained the viability and growth of these cells (figure 5). Notably, we did not observe any significant difference in the proliferation rates of laNK92-nLuc cells between hIL-2 NOG and hIL-15 NOG mice. This led us to conclude that the measured concentrations of hIL-2 and hIL-15 in mice plasma by Taconic Biosciences are more accurate than what is reported in the literature. In addition, we observed that mice injected IP with laNK92 cells exhibited signs of toxicity, as evidenced by significant weight loss approximately 30 days post-transplantation, ultimately resulting in death around 40 days. This observation aligns with the information provided by Taconic Biosciences, indicating the onset of graft-vs-host disease (GvHD) 4–6 weeks after the transplantation of immune cells, leading to subsequent death in certain NOG mouse models. This indicates that the window of opportunity for measuring the activity of BiKE:E5C1 in these two NK humanized models is limited to 30–40 days post-NK92 IP transplantation. Nevertheless, learning that both hIL-2 and hIL-15 NOG mice support the growth of laNK92 cells, we examined whether the viable laNK92 cells maintained their ability to kill the cancer cells in the presence of BiKE:E5C1. For this purpose, SKOV-3 cells were injected IP into mice to model metastatic ovarian cancer spreading to peritoneal



organs. The results of the *in vivo* studies demonstrated that BiKE:E5C1 activated laNK92-nLuc cells to release cytokines such as IFN- $\gamma$  and effector molecules, leading to clearance of cancer cells from the mice's peritoneal cavity in both hIL-2 NOG and hIL-15 NOG models (figures 6 and 7).

Overall, our data highlight two important points that need to be addressed in future studies. The first pertains to the limitation imposed by the immortality of the laNK92 cells, which accelerates the emergence of GvHD, thereby restricting the lifespan of mice to approximately 40 days. This renders it unfeasible to conduct long-term survival studies following the elimination of cancer. Therefore, the next logical step would be to use PB-NK cells, which have a short lifespan, to address this constraint. The second important point is that we have demonstrated the efficacy of BiKE:E5C1 in one tumor model. Thus, additional *in vivo* studies encompassing a broad spectrum of HER2-expressing tumors are necessary to further corroborate the observed *in vitro* anticancer efficacy data.

## CONCLUSIONS

The data in this manuscript demonstrate that BiKE:E5C1 can activate not only CD16-expressing NK cells but also macrophages, leading to the enhancement of their anti-cancer activity and acting as an effective immune cell engager. Since our CD16a-targeting platform recognizes a different epitope on CD16a antigen than IgG-based mAbs, it presents opportunities for both monotherapy and combination therapy with other antibody drugs. Considering that BiKE:E5C1 can activate NK cells to effectively eliminate trastuzumab-resistant as well as HER2-low cancer cells, it has the potential to compete with current FDA-approved antibodies such as Enhertu for treating a broad spectrum of HER2-expressing cancers. In conclusion, our data validate the functionality of the BiKE:E5C1 under *in vivo* conditions expanding the armamentarium for cancer immunotherapy.

**Acknowledgements** We would like to thank the NIH/NCI flow cytometry (P30CA072720-5924) shared resources of the Rutgers-Cancer Institute of New Jersey (NCI-designated Comprehensive Cancer Center).

**Contributors** SKN contributed to methodology, data acquisition, validation, formal analysis, investigation, writing, and visualization. GY and HO contributed to methodology, data acquisition, and visualization. MG-L, RIC, LGG and MM, were involved in methodology. AH contributed to conceptualization, methodology, validation, formal analysis, resources, writing, review and editing, visualization, supervision, project administration, and funding acquisition. AH is responsible for the overall content and serves as guarantor.

**Funding** This work was supported by grants from the New Jersey Health Foundation (PC95-20), NIH/NCI (R01CA251438), and NIH/NHLBI/Rutgers HealthAdvance joint program (U01HL150852).

**Disclaimer** The content is solely the responsibility of the authors and does not necessarily represent the official views of the National Institutes of Health or Taconic Biosciences.

**Competing interests** AH and SK are inventors named on a patent (W02023129819) that describes the BiKE technology. The intellectual property (IP) rights to the patented technology belong to Rutgers University.

**Patient consent for publication** Not applicable.

**Ethics approval** All *in vivo* studies were approved and conducted in accordance with the Institutional Animal Care and Use Committee of Rutgers University (Rutgers IACUC Protocol# PROTO999900106).

**Provenance and peer review** Not commissioned; externally peer reviewed.

**Data availability statement** All data relevant to the study are included in the article or uploaded as online supplemental information.

**Supplemental material** This content has been supplied by the author(s). It has not been vetted by BMJ Publishing Group Limited (BMJ) and may not have been peer-reviewed. Any opinions or recommendations discussed are solely those of the author(s) and are not endorsed by BMJ. BMJ disclaims all liability and responsibility arising from any reliance placed on the content. Where the content includes any translated material, BMJ does not warrant the accuracy and reliability of the translations (including but not limited to local regulations, clinical guidelines, terminology, drug names and drug dosages), and is not responsible for any error and/or omissions arising from translation and adaptation or otherwise.

**Open access** This is an open access article distributed in accordance with the Creative Commons Attribution Non Commercial (CC BY-NC 4.0) license, which permits others to distribute, remix, adapt, build upon this work non-commercially, and license their derivative works on different terms, provided the original work is properly cited, appropriate credit is given, any changes made indicated, and the use is non-commercial. See <http://creativecommons.org/licenses/by-nc/4.0/>.

## ORCID iDs

Shahryar Khoshtinat Nikkhai <http://orcid.org/0000-0002-7069-4111>

Lazaro Gil Gonzalez <http://orcid.org/0000-0002-3042-8919>

Arash Hatefi <http://orcid.org/0000-0003-4611-7469>

## REFERENCES

- Petricevic B, Laengle J, Singer J, *et al*. Trastuzumab mediates antibody-dependent cell-mediated cytotoxicity and Phagocytosis to the same extent in both adjuvant and metastatic Her2/neu breast cancer patients. *J Transl Med* 2013;11:307.
- Chenoweth AM, Wines BD, Anania JC, *et al*. Harnessing the immune system via Fc $\gamma$  receptors in immune therapy: a pathway to next-Gen mAbs. *Immunol Cell Biol* 2020;98:287–304.
- Bruhns P, Iannascoli B, England P, *et al*. Specificity and affinity of human Fc $\gamma$  receptors and their polymorphic variants for human IgG subclasses. *Blood* 2009;113:3716–25.
- Barb AW. Fc gamma receptor compositional heterogeneity: considerations for Immunotherapy development. *J Biol Chem* 2021;296:100057.
- Koene HR, Kleijer M, Algra J, *et al*. Fc gammaRIIIa-158V/F polymorphism influences the binding of IgG by natural killer cell FC gammaRIIIa, independently of the FC gammaRIIIa-48L/R/H phenotype. *Blood* 1997;90:1109–14.
- Rugo HS, Im S-A, Cardoso F, *et al*. Efficacy of Margetuximab vs Trastuzumab in patients with pretreated Erbb2-positive advanced breast cancer: a phase 3 randomized clinical trial. *JAMA Oncol* 2021;7:573–84.
- Muta T, Kurosaki T, Misulovin Z, *et al*. A 13-amino-acid motif in the cytoplasmic domain of Fc $\gamma$ RIIB modulates B-cell receptor signalling. *Nature* 1994;368:70–3.
- Ocaña-Guzman R, Vázquez-Bolaños L, Sada-Ovalle I. Receptors that inhibit macrophage activation: mechanisms and signals of regulation and tolerance. *J Immunol Res* 2018;2018:8695157.
- Morris AB, Farley CR, Pinelli DF, *et al*. Signaling through the inhibitory Fc receptor Fc $\gamma$ RIIB induces Cd8+ T cell apoptosis to limit T cell immunity. *Immunity* 2020;52:136–50.
- Nikkhai SK, Li G, Eleya S, *et al*. Bispecific killer cell Engager with high affinity and specificity toward Cd16A on NK cells for cancer Immunotherapy. *Front Immunol* 2022;13:1039969.
- Hatefi A, Nikkhai SK. Single-domain high affinity antibodies and methods of use thereof. *Patent Publication Number WO2023129819A2* 2023.
- Nikkhai SK, Heydarzadeh H, Vandavasi VG, *et al*. A high affinity and specificity anti-Her2 single-domain antibody (VHH) that targets Trastuzumab's EPITOPE with versatile biochemical, biological, and medical applications. *Immunol Res* 2024;72:103–18.
- Huang B, Sikorski R, Sampath P, *et al*. Modulation of Nkg2D-ligand cell surface expression enhances immune cell therapy of cancer. *J Immunother* 2011;34:289–96.
- Mensali N, Dillard P, Hebeisen M, *et al*. NK cells specifically TCR-dressed to kill cancer cells. *EBioMedicine* 2019;40:106–17.

- 15 Maki G, Klingemann HG, Martinson JA, *et al.* Factors regulating the cytotoxic activity of the human natural killer cell line, NK-92. *J Hematother Stem Cell Res* 2001;10:369–83.
- 16 Pályi-Krekk Z, Barok M, Isola J, *et al.* Hyaluronan-induced masking of ErbB2 and Cd44-enhanced Trastuzumab Internalisation in Trastuzumab resistant breast cancer. *Eur J Cancer* 2007;43:2423–33.
- 17 Malekshah OM, Sarkar S, Nomani A, *et al.* Bioengineered Adipose-derived stem cells for targeted enzyme-prodrug therapy of ovarian cancer intraperitoneal metastasis. *J Control Release* 2019;311–312:273–87.
- 18 Li G, Nikkhai SK, Hatefi A. Stem cell-assisted enzyme/prodrug therapy makes drug-resistant ovarian cancer cells vulnerable to natural killer cells through upregulation of Nkg2D ligands. *Med Oncol* 2023;40:110.
- 19 Gil Gonzalez L, Fernandez-Marrero Y, Norris PAA, *et al.* THP-1 cells Transduced with Cd16A utilize Fcγ receptor I and III in the Phagocytosis of IgG-sensitized human Erythrocytes and platelets. *PLoS One* 2022;17:e0278365.
- 20 Bertani FR, Mozetic P, Fioramonti M, *et al.* Classification of M1/M2-polarized human Macrophages by label-free Hyperspectral reflectance Confocal microscopy and multivariate analysis. *Sci Rep* 2017;7:8965.
- 21 Kilkeny C, Browne WJ, Cuthi I, *et al.* Improving Bioscience research reporting: the ARRIVE guidelines for reporting animal research. *Vet Clin Pathol* 2012;41:27–31.
- 22 Montecino-Rodriguez E, Dorshkind K. Use of Busulfan to condition mice for bone marrow transplantation. *STAR Protoc* 2020;1:100159.
- 23 Perussia B, Trinchieri G. Antibody 3G8, specific for the human neutrophil FC receptor, reacts with natural killer cells. *J Immunol* 1984;132:1410–5.
- 24 Gil Gonzalez L, Fernandez-Marrero Y, Norris PAA, *et al.* THP-1 cells Transduced with Cd16A utilize Fcγ receptor I and III in the Phagocytosis of IgG-sensitized human Erythrocytes and platelets. *PLoS One* 2022;17:e0278365.
- 25 Wolff AC, Hammond MEH, Hicks DG, *et al.* Recommendations for human Epidermal growth factor receptor 2 testing in breast cancer: American society of clinical oncology/college of American Pathologists clinical practice guideline update. *JCO* 2013;31:3997–4013.
- 26 Tam YK, Martinson JA, Doligosa K, *et al.* Ex vivo expansion of the highly cytotoxic human natural Killer-92 cell-line under current good manufacturing practice conditions for clinical adoptive cellular Immunotherapy. *Cytotherapy* 2003;5:259–72.
- 27 Nagashima S, Mailliard R, Kashii Y, *et al.* Stable Transduction of the Interleukin-2 gene into human natural killer cell lines and their Phenotypic and functional characterization in vitro and in vivo. *Blood* 1998;91:3850–61.
- 28 Törnroos H, Hägerstrand H, Lindqvist C. Culturing the human natural killer cell line NK-92 in Interleukin-2 and Interleukin-15 - implications for clinical trials. *Anticancer Res* 2019;39:107–12.
- 29 Katano I, Takahashi T, Ito R, *et al.* Predominant development of mature and functional human NK cells in a novel human IL-2-producing transgenic NOG Mouse. *J Immunol* 2015;194:3513–25.
- 30 Katano I, Nishime C, Ito R, *et al.* Long-term maintenance of peripheral blood derived human NK cells in a novel human IL-15-transgenic NOG Mouse. *Sci Rep* 2017;7:17230.
- 31 Morvan MG, Lanier LL. NK cells and cancer: you can teach innate cells new tricks. *Nat Rev Cancer* 2016;16:7–19.
- 32 de Haas M, Koene HR, Kleijer M, *et al.* A Triallelic FC gamma receptor type IIIA polymorphism influences the binding of human IgG by NK cell FC gamma RIIIa. *J Immunol* 1996;156:2948–55.
- 33 Pang Z, Wang Z, Li F, *et al.* Current progress of CAR-NK therapy in cancer treatment. *Cancers (Basel)* 2022;14:4318.
- 34 Zhang X, Guo Y, Ji Y, *et al.* Cytokine release syndrome after modified CAR-NK therapy in an advanced non-small cell lung cancer patient: A case report. *Cell Transplant* 2022;31:09636897221094244.
- 35 Zhang M, Lam KP, Xu S. Natural killer cell Engagers (Nkces): a new frontier in cancer Immunotherapy. *Front Immunol* 2023;14:1207276.

## Supplementary Materials

### **Bispecific Immune Cell Engager Enhances the Anticancer Activity of CD16+ NK Cells and Macrophages In Vitro, and Eliminates Cancer Metastasis in NK Humanized NOG Mice**

<sup>1</sup>Shahryar Khoshtinat Nikkhoi, <sup>1</sup>Ge Yang, <sup>1</sup>Hajar Owji, <sup>2</sup>Mayara Grizotte-Lake, <sup>3</sup>Rick I Cohen, <sup>4</sup>Lazaro Gil Gonzalez, <sup>1</sup>Mohammad Massumi, <sup>1,5</sup>Arash Hatefi\*

<sup>1</sup>Department of Pharmaceutics, Rutgers University, Piscataway, NJ, USA, 08854

<sup>2</sup>Taconic Biosciences, Inc., Rensselaer, NY, USA, 12144

<sup>3</sup>Department of Biomedical Engineering, Rutgers University, Piscataway, NJ, USA

<sup>4</sup>Keenan Research Centre for Biomedical Science, St. Michael's Hospital, Toronto, ON, Canada, M5B 1T8

<sup>5</sup>Cancer Pharmacology Program, Rutgers Cancer Institute of New Jersey, New Brunswick, NJ, USA, 08901



**Supplementary Method 1: *Cell culture and handling***

CD16+ natural killer cells from peripheral blood (PB-NK) were purchased (Lonza, Cat# 2W-501) and maintained in X-VIVOTM 15 Serum-free Hematopoietic Cell Medium (Lonza, 02-053Q) supplemented with 100 U/mL hIL-2 and hIL-15. THP-1-CD16A cells, while in a monocytic state, were maintained in RPMI1640 (ThermoFisher), supplemented with 10% FBS (ThermoFisher) and 2 mM Glutamine-alanine (ThermoFisher). They were seeded at a density of 0.2 million per ml complete media in a low adherent flask and passaged every 3 days. SKOV-3 cells (ATCC, HTB-77) were maintained in McCoy's 5A (Modified) Medium supplemented with 10% FBS. OVASC-1 cells were maintained in RPMI 1640 media supplemented with 15% FBS and 2.5 µg/ml insulin. JIMT-1 cells were cultured in DMEM/F-12, GlutaMAX™ supplemented with 10% FBS, 100 U/ml penicillin-streptomycin, and 10 µg/ml insulin. MDA-MB-231 and BT-474 cells were purchased from ATCC and cultured as per provided protocol.

**Supplementary Method 2: Expression and purification of BiKE:E5C1**

To express BiKE, 1 liter of LB media containing 50 µg/ml kanamycin was inoculated with 20 ml of overnight culture. Once the OD<sub>600</sub> reached 1.6, 0.5 mM IPTG was added to induce protein expression. The expression continued at 25°C for 18 hours and then bacterial culture was centrifuged at 10,000 g for 10 min at 4°C. The pellet was resuspended in 70 ml of lysis buffer (**Table 1**) and incubated at room temperature (RT) for 30 min while shaking. The bacterial suspension was then sonicated (5s on, 3s off, 70% amplitude) for 3 x 15 min on ice. Next, the cell debris was pelleted via centrifugation (40,000 g, 4°C, 45 min), the supernatant was loaded onto a Ni-NTA column and washed with 30 ml of wash buffer I and wash buffer II (**Table 1**). Before eluting the target protein, the column was washed twice with 25 ml of dulbecco's phosphate buffer saline (DPBS). To elute BiKE, 100 U/mL of WELQut protease (Thermo Scientific, Cat#EO0861) was added to the resin and incubated overnight at 4°C. The purity and concentration of the eluted protein was measured using SDS-PAGE and BCA assay, respectively.

**Table 1.** The compositions of buffers that were used for the purification of the BiKE:E5C1 from bacterial lysate.

Reagents/Buffers	Lysis buffer	Wash Buffer I	Wash Buffer II	WELQut
MiliQ water	Yes	Yes	Yes	Yes
Tris	50mM (6.057g/L)	50mM (6.057g/L)	50mM (6.057g/L)	--
Na <sub>2</sub> HPO <sub>4</sub>	100mM (7.1g/L)	100mM (7.1g/L)	100mM (7.1g/L)	--
NaCl	250mM (14.6g/L)	500mM (29.2g/L)	1M (58.4g/L)	250mM (14.6g/L)
KCl	--	--	--	250mM

				(18.64g/L)
Imidazole	5 mM 0.33g/L	10 mM 0.66g/L	10 mM 0.66g/L	--
EDTA	1mM (0.292g/L)	--	--	--
Glycerol	5% (v/v)	5% (v/v)	5% (v/v)	--
PBS (solvent)	--	--	--	Yes
Triton X-100	1% (10mL/L)	0.2% (2mL/L)	--	--
PMSF	1mM	--	--	--
Lysozyme	0.2mg/mL	--	--	--
RNase A	10 ug/mL	--	--	--
DNase I	5 ug/mL	--	--	--
pH	7.0	7.5	7.5	7.5



**Supplementary Method 3:** *Measurement of the degranulation of laNK92 cells using surfaced CD107a*

SKOV-3 cells were seeded in a 96-well plate at the density of  $10^4$  cells per well and incubated overnight. The next day, a serial dilution of BiKE, spanning from 0 to 100 nM, was added into the wells and incubated for 30 minutes at 37°C. Then, laNK92 (GFP+) cells were added to SKOV-3 cells at an E:T ratio of 4. This cell combination was then incubated for 3 hours at 37°C. Following this stage, a human LAMP-1/CD107a APC-conjugated Antibody (R&D Systems, Cat#IC4800A) was added to the mix and incubated for 1 h. Subsequently, the plate was centrifuged, the supernatant was removed, and a double washing step was executed to eliminate excess antibody. A Beckman Coulter CytoFLEX Cytometer was then used for data acquisition. For data analysis, the GFP+ (laNK92) subset was gated to distinguish between the effector and target cells. In the final analytical step, the mean fluorescent intensity (MFI) of surfaced CD107a molecules within the GFP+ cell population was quantified.

**Supplementary Method 4:** *Evaluation of the impact of hIL-2 and hIL-15 on laNK92 cytotoxicity*

One day prior to the assay, 10,000 SKOV-3 cells were seeded. The next day, the cells were incubated with BiKE:E5C1 (100 nM) for 30 minutes at 37°C. This was followed by the addition of laNK92 cells at E:T ratios of 0, 1, 2, and 4. In the case of the BiKE:E5C1 kill curve, SKOV-3 cells were seeded and then treated with varying BiKE:E5C1 concentrations ranging from 0 to 100 nM for 30 minutes at 37°C. After this, laNK92 cells were added at an E:T ratio of 4. Following a 4-hour incubation period, we assessed the cell viability using alamarBlue cytotoxicity kit and protocol.

**Supplementary Method 5: Measurement of cytokine release**

SKOV-3 cells were seeded in a 96-well plate at the density of  $10^4$  cells per well. The next day, 100 nM BiKE:E5C1 was added to the plate and incubated at 37°C for 30 min. Next, PB-NK or laNK92 cells were added at E:T ratio of 4. After 24 h, plates were centrifuged at 2000 g for 10 min to pellet the cells. Then, the supernatant was transferred into a non-treated 96-well plate. The amounts of TNF- $\alpha$  and IFN- $\gamma$  cytokines were measured using DuoSet ELISA Kit (R&D Systems, USA). The data are presented as mean  $\pm$  SD (n=3).

In in vivo study, the concentrations of IFN- $\gamma$  within murine blood were measured. Blood samples were collected one week after treatment, using heparinized microhematocrit tubes (Fisher Scientific, Cat#22-362566). Following collection, blood samples were centrifuged at 10,000 g for 10 minutes at 4°C. The concentration of IFN- $\gamma$  was measured using the DuoSet ELISA Kit as mentioned above. The data are presented as mean $\pm$ s.d. (n=3).

**Supplementary Method 6:** *Genetic engineering and characterization of NK92-nLuc cells*

To engineer laNK92-nluc cells, laNK92 cells were passaged at a low density of 50,000 cells/ml supplemented with 600 IU/ml of human interleukin 2 (hIL-2) (PeproTech) and then processed using the buffers from the kit associated with Neon™ NxT electroporation system (ThermoFisher Scientific). On the day of electroporation, cells were harvested and subjected to three consecutive washes with Opti-MEM (Invitrogen). Following the final wash, cells were resuspended in a buffer solution at a concentration of  $4 \times 10^7$  cells in 850  $\mu$ l of O buffer containing 0.1% CD buffer. Subsequently, 85  $\mu$ l of this cell suspension was mixed with 15  $\mu$ l of plasmids, consisting of 5  $\mu$ g of piggybac transposase and 10  $\mu$ g of pb-nLuc. Electroporation was carried out using the Neon™ NxT electroporation system with two pulses: an initial pulse of 1650 V for 20 ms followed by a second pulse of 500 V for 100 ms (please see PMID: 31114587). Immediately post-electroporation, cells were resuspended in NK92 culture media supplemented with 600 IU/ml of hIL-2 and incubated for three days. Then, 200  $\mu$ g/ml of hygromycin B (Gibco) was added to the culture media to select for nanoluciferase-expressing laNK92 cells (laNK92-nLuc). The selection process was maintained for a duration of three weeks.

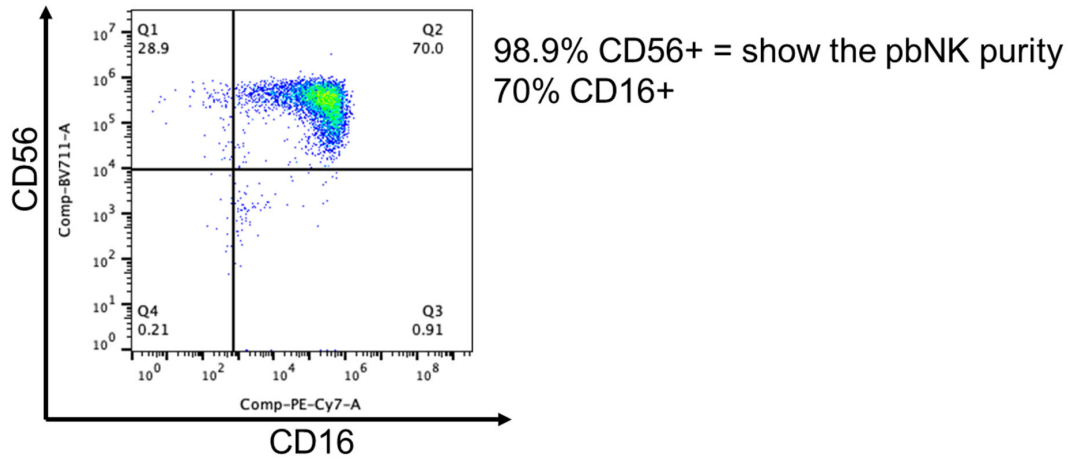
To compare the proliferation rate of the laNK92 cells with laNK92-nluc cells, they were collected and washed with DPBS. Subsequently, cells were fixed using a 3.7% formaldehyde solution for a duration of 15 minutes, followed by a dual washing step with DPBS. The fixed cells were then rendered permeable through treatment with 1% Triton X-100 for 15 minutes followed by a dual washing sequence. The resultant permeabilized cells were resuspended in an intracellular staining solution comprising DPBS, 2% FBS, and 0.1% Triton-X100. To stain the cells, they were incubated overnight with APC-conjugated anti-Ki-67 antibody (Biolegend) at 4°C. Upon

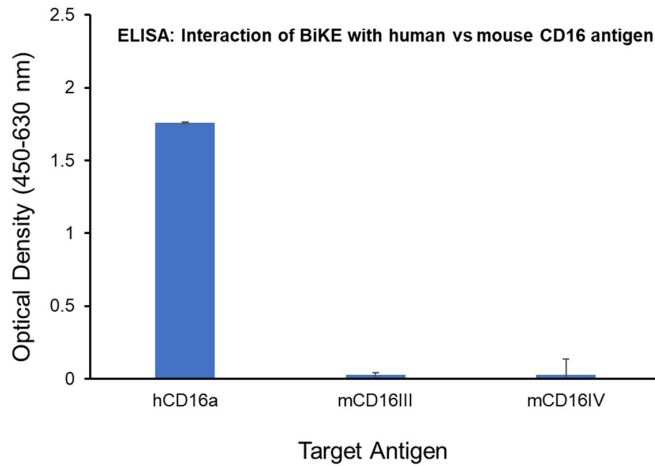


completion of the staining, cells were washed three times and then analyzed using a Beckman Coulter Cytoflex flow cytometer at Rutgers Flow Cytometry Core Facility.

To compare the proliferation rates of laNK92 and laNK92-nLuc cells, the Ki-67 proliferation index was measured using flow cytometry and established protocols (please see PMID: 28446615).

**Supplementary Fig. 1:** Characterization of the PB-NK cells in terms of CD56 and CD16 receptor expression levels using flow cytometry. The data show the purity of the PB-NK cells is ~99%, and 70% of the PB-NK cells used in this study expressed CD16 receptors.





**Supplementary Fig. 2:** Characterization of BiKE:E5C1 and its interaction with mouse CD16 antigen (mCD16III and mCD16IV) using ELISA. In this experiment, a 96-well ELISA plate was coated with human CD16a, mouse CD16 III and CD16 IV proteins at concentrations of 1  $\mu\text{g}/\text{mL}$  in coating buffer. After an overnight incubation at 4°C, the coating solutions were discarded, and the plates were washed once with DPBS containing 0.05% Tween-20 (PDBS-T). Nonspecific binding sites were blocked by adding 200  $\mu\text{L}$  of blocking buffer (1% BSA in DPBS) per well and incubating at room temperature for 2 hours. Next, BiKE:E5C1, prepared at concentration of 1  $\mu\text{g}/\text{mL}$  in 0.5% BSA in DPBS, was added (100  $\mu\text{L}/\text{well}$ ). After 1 hour of incubation at room temperature while shaking at 700 rpm, the plate was washed thrice with PBS-T. Then, 100  $\mu\text{L}$  of anti-cMyc HRP-conjugated secondary antibody was added and incubated for 1 hour while shaking at 700 rpm. After additional PBS-T washing, 50  $\mu\text{L}$  of 3,3',5,5'-Tetramethylbenzidine (TMB) substrate solution was added to initiate the colorimetric reaction, which was allowed to proceed for 15 minutes at room temperature. The reaction was stopped by adding 50  $\mu\text{L}$  of 2M sulfuric acid to each well. Absorbance measurements were taken at 450 nm and 630 nm (as a reference) wavelength using Tecan Infinite<sup>®</sup> M200 PRO plate reader.

# Bispecific Killer Cell Engager Activates Natural Killer Cells to Eliminate Cancer Metastasis in NK Humanized NOG Mice

**Authors:** Shahryar K. Nikkhoi, Ge Yang, Hajar Owji, Mayara Grizotte-Lake, Rick I Cohen, <sup>4</sup>Lazaro G. Gonzalez, Mohammad Massumi, Arash Hatefi

**Correspondence:** ahatefi@pharmacy.Rutgers.edu

